

SPIRAL ARMS IN GALAXIES  
WITH COUNTER-ROTATING STELLAR DISKS

s. Howard

Jet Propulsion Laboratory, California Institute of Technology  
4800 Oak Grove Drive, Pasadena, California 91109  
Electronic mail: showard@smtp.gsfc.nasa.gov

M.T. Carini

Center for Automated Space Studies  
Department of Physics and Astronomy  
Western Kentucky University, Bowling Green, KY 42101-3576  
Electronic mail: carini@wku.edu

G.G. Byrd

Department of Physics and Astronomy  
University of Alabama, Tuscaloosa, Alabama 35487-0324  
Electronic mail: byrd@possum.astr.ua.edu

S. Lester

Louisiana State University, Baton Rouge, Louisiana 70803  
Electronic mail: lester@rouge.phys.lsu.edu

*Received* .....

*Accepted* .....

## ABSTRACT

Spectroscopic observations by Rubin and others indicate that the S type galaxies NGC 4550, NGC 7217 and NGC 4138 have two-way disks with a substantial portion of the stellar disk orbiting opposite the direction of the rest. In 1977, Kalnajs found in analytical work that a particular two-way disk model was less susceptible to two-fold bar instabilities even in the absence of any inert stabilizing halo. This raised hopes of a non-halo mechanism to stabilize disks. However, in 1978, Zang and Hohl found via simulations that one-fold instabilities were enhanced in a two-way disk with no halo. Zang and Hohl's simulations were of an isolated disk with a fairly flat rotation curve. In recent simulations, Sellwood and Merritt find that the one-sided instability is enhanced in simulations of no halo Kuz'man/Toomre disks but that a stable model parameter range does exist. Kuz'man/Toomre disks have rising and then falling rotation curves. The observed two-way galaxies have flat rotation curves over most of their disks. Using a self-gravitating disk with a flat rotation curve, we redo Zang and Hohl's isolated simulations but with more particles plus varying amounts of an inert "halo" component. We confirm the instability of a disk with no halo and find that an inert halo equal to the two-way disk will stabilize against both one and two sided disturbances. Since small companions should frequently perturb disk galaxies, we conduct a variety of simulations of the spiral arm patterns created by such passages comparing two-way to one-way disks. With the same amount of halo, tidal spiral arm patterns in two-way disks are more symmetric, smoother and weaker than in one-way disks. Galaxies with these characteristics may be more likely observational candidates in the search for two-way stellar disks.

## I. INTRODUCTION

### *1.1 Galaxies with Substantial Counter-rotating Stellar Disks*

Recently a number of galaxies have been discovered in which a substantial portion of the stellar disk is counter-rotating relative to the rest of the stellar disk. Spectroscopic observations indicate that the SO galaxy NGC 4550 is a two-way disk galaxy with a substantial portion of the stellar disk orbiting opposite the direction of the rest (Rubin

1993, Rubin, Graham and Kenney 1992, Rix, Franx, Fisher and Illingworth 1992). Via spectroscopic observations, the Sab galaxy NGC 7217 has also been shown to have at least 30 percent of the stars in its disk two way relative to the rest over a substantial portion of the disk (Merrifield and Kuijken 1994). NGC 4138 (Jore, Brocils and Haynes 1995, 1996) has been found to have at least 20 percent of its stellar disk to be counter-rotating.

The estimated portion of the disk which is counter-rotating in the examples above is based on ratios of line strengths. Since the components are probably of different ages and metallicities which would also affect line strengths, the actual mass-fraction which is counter-rotating could be larger than stated. Because galaxies with substantial stellar counter-rotating disks have now been found to exist, theoretical studies of the dynamical stability and morphology of two-way stellar disks have become more interesting since the gravitation of the counter-rotating component should be significant. Merrifield and Kuijken (1994) suggest that because the detection of galaxies with substantial stellar counter-rotating disks is difficult, these may be more common among galaxies than one would think from the few examples found so far. This paper studies such galaxies via simulations to determine which kinds of galaxies might be good candidates for these difficult observations. The our simulations are not aimed directly toward determining how these galaxies may have formed. See Thakar and Ryden 1996) for recent simulations of possible formation processes. Our results will however be useful in the determination of how common these galaxies may be which will have a strong indirect effect on judging what is the best formation mechanism.

Bertola, Buson and Zeilinger (1992) divide counter-rotating disk galaxies into three groups: (1) The above group (NGC 4550, NGC 7217 and NGC 4138) in which substantial portions of the stellar disk orbit opposite the rest of the stellar disk. (2) Galaxies with counter-rotating disks where the gas disk rotates opposite the old stellar disk. Examples are NGC 3626 (Ciri, Bettoni and Galletta 1995) and several SO galaxies (Galletta 1987, Bertola, Buson and Zeilinger 1992). (3) Cases where one portion of the gaseous disk orbits opposite another (e.g. NGC 4386, Braun, Walterbos, and Kennicutt 1992, Rubin, 1994, Walterbos, Braun and Kennicutt 1994). We will restrict our simulations to the extreme case (1) where the two-way condition extends over the entire disk in the gravitationally dominant

stellar component and the oppositely orbiting portions are equal in mass. We do this for simplicity and because gravitational effects will be largest in case (1). If there are interesting dynamical effects, they should show up and determine whether or not further work is justified.

### *1.2 Past Simulations and the Hope of “No-Halo Stabilization”*

In the 1970's, self-gravitating simulations of galaxy disks showed a disturbing propensity to two-fold (bar) instabilities creating velocity dispersions far in excess of those observed in the Galaxy (e.g. Hohl 1971, Miller 1971). On the basis of simulations, Ostriker and Peebles (1973) and many others since have argued that a previously undetected high velocity dispersion halo is needed to stabilize the disks of spiral galaxies. Kalnajs (1977) found in analytical work that two-way disks were less susceptible to two-fold bar instabilities even in the absence of any stabilizing halo. Kalnajs suggested that “reversing the angular momenta of some stars provides a more effective way of stabilizing a disk than just pretending they are part of an immobile halo.” Via simulations, Zang and Hohl (1978) confirmed that the stability-enhancing effects of two-way disks against bar formation are true for an isochrone disk and for a fairly flat rotation curve disk resembling the Schmidt model of our Galaxy.

The hope had been raised that there may be no need for extended halos to stabilize disk galaxies. However, Zang and Hohl (1978) found that an  $m = 1$  “lop-sided” instability was enhanced for both the isochrone and flat “Schmidt” disks as the fraction of disk stars which orbited opposite the majority was increased. A number of authors have analytically verified Zang and Hohl’s simulation results for a variety of models e.g. Sawamura (1988) for weakly shearing disks and Merritt and Stiavelli (1990) for oblate spheroids. Most recently, Lovelace, Jore and Haynes (1996) have analytically evaluated the instability for a variety of cases of counter-rotating gas or stars. In simulations, Sellwood and Merritt (1994) also found for Kuz’mán/Toomre disks that counter rotation enhanced the  $m=1$  instability. Sellwood and Merritt (1994) also studied bending instabilities. These instabilities eventually caused the disk to thicken to a certain degree largely independent of the initial thickness (See Sellwood and Merritt’s Figure 7). Sellwood and Merritt were successful in finding a

thin model with  $Q$  of 1.7 which survives for a large number of dynamical times in the complete absence of a halo. They suggest that this model might be appropriate for NGC 4550.

### *1.3 New Simulations of Two-way Disk Tidal Arm Morphology*

The group (1) counter-rotating stellar **disk** galaxies discovered so far have rather flat rotation curves. Rubin et al (1992) describe the rotation curve of the NGC 4550 disk containing the two-way component as “rising to 120 km/s at 5 arc seconds and constant beyond” to 30 arc seconds. As described in the observational papers cited above, the counter-rotating galaxies NGC 7217, NGC 4138 and NGC 3593 also have flat rotation curves over most of their optical disks. The Kuz'man/Toomre disk simulations of Sellwood and Merritt (1994, see their Figure 1) have rising and then falling rotation curves. To conform to the observed properties of the counter-rotating galaxies cited above more simulations with flat rotation curves are needed. In the present paper, we discuss new isolated simulations similar to the flat rotation curve disk stability simulations of Zang and Hohl (1978) but with more particles and better display of the disk morphology. Also, since the Zang and Hohl simulations had no halo, we carry out the simulations with varying amounts of an inert halo added to ascertain how much halo would be needed for stabilization of counter-rotating stellar disks against one-fold disturbances.

Isolated simulations are somewhat artificial since the perturbations arise via numerical effects in the model. The stability of self-gravitational disks of galaxies is actually “tested” in nature via frequent tidal perturbations by a few large and many small companions. These perturbations can be very effective and are possibly the major way that global spiral arm patterns are created in galaxies” (Byrd and Howard 1992). Since galaxies with substantial counter-rotating stellar disks have been shown to exist and may even be fairly common, we will also simulate the morphological response of self-gravitating two-way and one-way disks to tidal perturbations by a variety of companions. If there are systematic differences between the shapes of tidally created arms in two-way versus one-way stellar disks this may suggest which type galaxies are likely candidates for the difficult observations in search of counter-rotating stellar components.

## 11. SIMULATION MODEL

The simulation code is a fully self-gravitating polar grid code. The original version was written by Miller (1976) as probably the first polar grid n-body code used for galaxy simulations. The present code is a greatly modified descendant which has been tested against independently written polar and Cartesian grid codes (for details see Thomasson 1989, Howard 1989, Howard and Byrd 1990, Howard et al. 1993).

As mentioned earlier-, the counter-rotating stellar disk examples have flat rotation curves. The particular self-gravitating disk with a flat rotation curve that we use is a finite-radius Mestel (1963) disk. This disk has an analytically finite radius,  $R_g$ , with a flat rotation curve of velocity,  $V_g$ , to the disk edge. One crossing time for the galaxy is defined to be  $R_g/V_g$  and is set to 50 time steps in the simulation. Taking the disk radius to be 20 kpc with a disk orbital speed of 200 km/s, the length of a time step in millions of years is  $20 R_g/V_g$  or about two million years. Our simulations typically cover 1000 time steps or about two billion years, a reasonable length of time to test stability.

Besides the self-gravitating disk, the model contains an inert, non-self-gravitating ‘halo’ component. This inert component may be due to a halo and/or bulge which has a large velocity dispersion and is thus very stable or insensitive to perturbations. The halo component’s effect on the disk is specified by the halo-to-disk ratio, “H/D,” which is the ratio of the relative contributions of the halo and the disk to the gravitational acceleration of an orbiting disk particle toward the center of the initial disk. For the isolated simulations, we assumed the disks to have 180,000 star particles. Zang and Hohl (1978) had 50,000 particles. We make the extreme assumption of equal numbers in each of the two-way stellar components. The local stellar velocity dispersion is set so that Toomre’s axisymmetric stability criterion,  $Q$ , is equal to 1.0 for both one-way and two-way disks. However, it should be noted that unavoidable effects of softening of the force in this and other types of n-body programs raise the net  $Q$  of the disk to  $\sim 1.5$  with larger values in the central portions or near the edge of the disk (Byrd et al. 1986, Byrd 1995). This softening of the force law also mimics the effect of a finite disk thickness.

Our main interest is in disk-plane arm morphology. The particles in our simulations are constrained to move within a two-dimensional disk. This saves computation time and increases the number of particles possible in a simulation. Realism of in-plane features is not affected much by disk warps since in-plane accelerations change only as the cosine of the bending angle. Sellwood and Merritt's (1994) simulations do show some bending instabilities but not to a degree that the in-plane forces will be changed significantly. Comparing two and three dimensional simulations of M51 after a single passage of a perturber (Howard and Byrd 1990 and Byrd and Salo 1996), no real effects on a change from two to three dimensions are seen in a face-on view of the disk-plane arm structure.

We checked carefully to see that the code was functioning as it should. An interesting, after-the-fact test involved having the companion orbit past the disk in two otherwise identical orbits of opposite sense. In a one-way disk the resulting morphologies for these two passages are quite different. But for a two-way disk, the resulting tidal morphologies were identical except that they are mirror images of one another at every time step. For more details about the code see Byrd and Howard (1992) and references therein.

### 111. TWO-WAY VERSUS ONE-WAY ISOLATED DISKS

Our use of 180,000 stars (rather than the billions found in actual galaxies) results in small statistical perturbations whose effects we study in isolated disks to indicate the stability of the disk. We compare simulations of one-way disks versus two-way disks, and we study evolution at several H/D ratios rather than zero alone as in other studies (e.g. Zang and Hohl 1978, Sellwood and Merritt 1994).

The morphological evolution of these comparative simulations are displayed in an identical manner in the figures. We attempted to improve the display over previous studies so that the main conclusions of this article are made clear by simple comparison of the simulation images. Increasing particle number or density is indicated by increasing darkness except in the outer portions where single particles are shown. The method of the display is described in more detail in the Appendix. Table I lists the simulations carried out for this article. Figure number references are given along with the parameters of the simulations.

The evolution of an isolated two-way disk with  $H/I = 1$  is shown in Figure 1. The changes with time in an isolated one-way  $H/I = 0$  disk are shown in Figure 2. The initial, circular disk is shown on the upper left in both Figures to establish the scale and time sequence. In neither case is the disk stable. While we expect the one-way disk with no halo to be unstable, counter-rotation evidently does not contribute to stability of a two-way disk. It is very clear in these two figures neither is stable and that the isolated two-way disk (Figure 1) behaves in a manner different from the corresponding isolated one-way disk (Figure 2). The two-way disk shows its instability in a one-sided manner just as expected from Zang and Hohl (1978). The one-way Figure 2 disk shows more two-fold features.

In general, increasing the halo's contribution stabilizes both kinds of disks against perturbations to about the same degree. Our simulations indicate that  $H/I = 0.5$  is just on the stabilization side of the boundary of halo stabilization of both one-way and two-way disks. As shown in Figure 3 of a two way disk,  $H/I$  of 0.5 suppresses the violent instabilities seen if no halo is present. Although, there is leakage from the edge and a weak ring is cast off in the last frame, the basic structure of the disk as seen in the shading from gray in the outer parts to black in the center is the same in the last frame as in the first. The results are very similar for a one-way disk. For  $H/I$  of 1 or larger, isolated two-way disks are quite stable as are one-way disks (See Howard et al. 1993, Figure 1). We emphasize that these disks with this much halo are very stable against the formation of bars.

#### IV. TWO-WAY VERSUS ONE-WAY TIDALLY PERTURBED DISKS

We also simulate tidally perturbed two-way disks. Here we investigate whether typical spiral galaxies would show different arm morphologic if they had two-way stellar disks rather than one-way disks. Our emphasis will not be on extremely violent perturbations because such encounters are more rare than smaller perturbations and because the galaxy structure is disrupted so much by these passages that diagnosing systematic differences would be doubtful both in the simulations and in the observations. We are interested in whether images of disk galaxies at wavelengths which show the underlying stellar disks (e.g.



1 band) may be usable to judge whether difficult absorption line spectroscopy for counter-rotation is justified. An inert, softened perturber is initially placed in a zero-energy orbit far enough away to ensure insignificant tidal effects. Different pericenter distances relative to the initial disk radius are simulated with the tidal effects appearing as close approach occurs. The companion orbits in the disk plane. Again, parameters of the simulations are listed with figure numbers in Table 1.

First we consider distant perturbations of two-way and one-way disks by a small mass perturber. These should be the most numerous type. Figure 4a,b shows the time sequence of a two-way stellar disk galaxy with  $H/D = 1$  perturbed by a low mass ( $0.1$  galaxy mass) companion passing clockwise at two disk radii. The companion is seen as a darker dot in some of the frames. Since the details of the arm morphology are important in our tidally perturbed models, we adopt a procedure to show the tidal arms more clearly on the printed illustrations. Figure 4b shows the same simulation of a perturbed two-way disk as in Figure 4a but with the morphology delineated by non-colliding "star" particles which have no initial velocity dispersion. As the reader can see, these particles show the same arm morphology as Figure 4a but the arms are sharper, darker and thus visible in the printed illustration. We will show this type display for the tidal arms of our two-way disk simulations.

We show a mosaic from an otherwise identical one-way perturbed disk simulation in Figure 5. The perturber passes in the same direction (sense) as the disk spins in this one-way simulation. We also simulated the effects of an opposite sense perturber on a one-way disk at this distance of close approach. The effects of an opposite sense perturber on a one-way disk are not very large so we do not show a time sequence for this case (see Table I). We refer the reader to Howard et al. (1993) for a video illustration of a two disk radius opposite sense encounter for the one-way disk (encounter number 40).

Comparing the two-way Figure 4 and one-way Figure 5 disks, the initial effects (first four frames left to right) of the perturber on the edge of the two-way disk in Figure 4 are significantly different from the corresponding frames of the perturbed one-way disk in

Figure 5. The disturbance in the disk is weaker and more symmetric. In later frames 5 through 7), we note that the two-way disk at 111s are weaker, smoother and more tightly wound than the perturbed 011(1-way disk. In frames 8 till 10), because the perturber has lost orbital energy to the one-way disk, it has returned for a second close passage. Dynamically, this greater loss of perturber energy and possible capture is another difference between the one-way and two-way disks. The final frames of the two-way Figure 4 disk show a symmetric, smooth disk galaxy with tightly-coiled narrow arms in contrast to the one-way galaxy. Galaxies with this morphology might be good observational candidates for two-way disks.

Next we will consider close perturbations by small mass companions. Figure 6a,b shows a two-way disk perturbed by a 0.1 mass perturber which grazes the disk. Compare this to Figure 7 which shows a similar encounter for a one-way disk with the companion passing in the same sense as the disk spin. When the companion leaves the two-way disk after close approach, the smooth two-armed tightly wound pattern appears in Figure 6's frames 6, 7, and 8 which resembles the pattern in the more weakly perturbed two-way disk of Figure 4a,b. As in the previous comparison, this more strongly perturbed two-way disk is more symmetric and the arms more tightly coiled than in the corresponding close passage one-way disk (Figure 7).

Figure 8a,b shows a fairly gentle perturbation of a two-way disk by a half-galaxy mass disturber passing at two disk radii. While such encounters will be less frequent than those we have already discussed, some distinctive feature combinations are present in the early stages that distinguish two-way from one-way disks. The patterns for this two-way disk perturbation are superpositions of the features seen in the perturbation of one-way disks by companions orbiting opposite to and in the same sense as the disk spin. For images of corresponding one-way disk encounters, we refer the reader to encounters number 5 and 41 in the Howard et al (1993) simulation survey video. A distinctive feature of same-sense perturbations of one-way disks is a pair of 100SC tidal arms that coil up as time passes. These are also seen in frames 3, 4, 5 and 6 of the Figure 8a,b two-way disk. A distinctive feature of strong encounters with a perturber opposite the disk sense is a distinctive set

of “ripples” in a one way disk on the side toward the perturber (See Figure 2a of Howard et al. 1993). The ripples are also seen in frames 3 and 4 of the Figure 8a,b two-way disk. A perturbed galaxy with the combination of loose arms and ripples would be a good two-way disk candidate.

## V. DISCUSSION

The observed two-way stellar disk galaxies have flat rotation curves. We thus simulate isolated two-way flat rotation curve disks in a confirmation and extension of Zang and Hohl’s (1978) study. Similar to Zang and Hohl’s results, our finite two-way Mestel disks with no halo are just as violently unstable as one-way disks with  $H/D = 1$  halo. There is a difference in that the two-way disks have a one-sided instability while the one-way disks show a two-sided instability. Going beyond Zang and Hohl (1978), we do isolated simulations with different amounts of halo and find that the halo parameter  $H/D$  value seems to be equally stabilizing for both one-way and two-way simulations. Inert “halos” comparable to the disk are required to stabilize two-way as well as one-way disks. Thus we suspect that the observed two-way disk galaxies have some sort of stabilizing inert component. In our simulations, an  $H/D$  of at least one or greater is sufficient to stabilize the two-way stellar disk with equal components.

Since the number of galaxies increases rapidly as galaxy mass is decreased, tidal perturbation of disk galaxies by small mass companions is rather frequent. We thus simulate the effects of distant ( $2$  disk radii), nearby (disk grazing) and small ( $1/10$  galaxy) mass perturbers on two-way stellar disks and compare them to those in one-way disks. The initial effects of the small mass perturber on the edge of the two-way disk are significantly different from the corresponding frames of the perturbed one-way disk. The disturbance in the two-way disk is weaker and more symmetric. In later frames, we note that the two-way disk arms are weaker, smoother and more tightly wound than the perturbed one-way disk. The final frames of the two-way disk show a symmetric, smooth disk galaxy with tightly-coiled narrow arms. The anemic class of spirals proposed by van den Bergh (1978) which show smooth spiral arms could be good candidates in the observational search for

other galaxies with counter-rotating stellar disks.

Perturbations of a two-way **disk** by more massive ( $1/2$  galaxy) but distant ( $2$  **disk** radii) perturbers **Should** be less frequent than **Such** passages by small mass perturbers. For a distant more massive perturber, some distinctive feature combinations are present in the early stages that distinguish two-way from one-way **disks**. The patterns are superpositions of the ripples and loose **al**'ills seen in the perturbation of one-way **disks** by companions orbiting opposite to and in the same sense as the **disk** spin. While these **features** are present for only a short interval, they are distinctive and could indicate substantial counter-rotating disk galaxies in particular encounters and times.

GB was supported by NSF EPSCoR Grant RII 8996152 and NSF Grant AST 9014137. S1, was supported by the NSF Grant AST 9300413 (Summer REU program).

TABLE 1  
LIST OF SIMULATION PARAMETERS

Figure Number	H/D	Perturber Distance	Portion Counter Rotating	Perturber vs. Disk Sense
1	0.0	Isolated	0.5	Isolated
2	0.0	Isolated	0.0	Isolated
Not shown	1.0	Isolated	0.5	Isolated
Not shown	1.0	Isolated	0.0	Isolated
3	0.5	Isolated	0.5	Isolated
Not shown	0.5	Isolated	0.0	Isolated
4a,b	1.0	2 disk radii	0.5	Undefined
5	1.0	2 disk radii	0.0	Same
Not shown	1.0	2 disk radii	0.0	Opposite
6a,b	1.0	1 disk radius	0.5	Undefined
7	1.0	1 disk radius	0.0	Same
8	1.0	2 disk radii	0.5	Undefined

Notes: Simulations are carried out for 900 time steps for the one-way disk simulations, 1000 steps for the two-way disks. The perturber mass is 0.1 galaxy mass for all the non-isolated simulations except for the Figure 8 encounter which had a 0.5 galaxy mass perturber.

## Appendix

In this article the main conclusion becomes clear by simple examination of the simulation images. We describe our method of display here in more detail. Since we have so many particles (1 80,000) it is impossible to plot them individually without getting a blob of superposed points in the central disk regions. The usual procedure of displaying only a subset of points results in lost information. Instead, we take the positions of the points and construct a 256 x 256 spatial grid and determine how many points are in each cell of the grid. The dimensions of the grid are four initial disk radii square. We then display the cells as shaded squares from light to dark as the particle number increases. No information is lost about the inner disk particle distribution. The particle density is sparse enough in the outer edges of the disk so that they are seen as tiny, individual, lightly-shaded squares.

The images reproduced here were taken from 256 x 256 arrays of floating-point numbers which ranged in value from zero to approximately 60,000 per cell. The arrays were scaled by the number 256/60000 to provide proper darkness contrast between inner and outer structure. The cells with only one particle were set to approximately 2200 by adding this number to all non-zero cells. This assured that single-particle cells were slightly darker than the surrounding empty cells so as to be easily seen. The white areas in the center correspond to an inert center in the n-body model.

The images were displayed using the IDL routines "tv" and "congrid," and each image was resized for display. The images were loaded with a standard black and white linear table. In order to improve the color contrast, the color table of each image was reversed and stretched by xloadct from the IDL widget library. The bottom and top stretch bars of xloadct were set to zero and thirty, respectively. Darker shading corresponds to areas which represent larger mass. Lighter shading corresponds to areas of low mass.

## References

- Bertola, F. Buson, L. M. and Zeilinger, W. W. 1992 ApJ 401, 179.
- Braun, R., Walterbos, R. A. M. and Kennicutt, R. C. Jr. 1992 Nature 360, 442.
- Byrd, G. 1995, Proceedings of the *Waves in Astrophysics* conference. Editors J. H. Hunter and R. B. Wilson. Annals of the New York Academy of Sciences, Vol. 773, p. 302.
- Byrd, G. and Howard, S. 1992 AJ 103, 1089.
- Byrd, G. and Salo, H. 1995 Astron. Letters and Communications 31, 193.
- Byrd, G., Valtonen, M. J., Sundelius, B. and Valtaoja, L. 1986 Astron. and Astrophysics 166, 75.
- Ciri, R., Bettoni, D. & Galletta, G. 1995 Nature, 375, 661.
- Galletta, G. 1987 ApJ, 318, 531
- Hohl, F. 1971 ApJ 168, 343.
- Howard, S. 1989 Dissertation, Georgia State University.
- Howard, S. and Byrd, G. G. 1990 AJ, 99, 1798.
- Howard, S., Keel, W. C., Byrd, G., and Burke, J. 1993 ApJ, 417, 502.
- Jore, K. P., Brocils, A. H., & Haynes, M. 1995 BAAS 27, 1442.
- Jore, K. P., Brocils, A. H., and Haynes, M. P. 1996 AJ submitted.
- Kalnajs, A. J. 1977 ApJ 212, 627.
- Lovell, R. V. E., Jore, K. P. and M. P. Haynes 1996 preprint.
- Merrifield, M. R. and Kuijken, K. 1994 ApJ 432, 575.
- Mestel, L. 1963 MNRAS 126, 553.

- Miller, R. 11. 1971 *Astrophysics and Space Science* 14, 73.
- Ostriker, J. D. and Peebles, P. J. E. 1973 *ApJ* 186, 467.
- Rix, 11. -W., Franx, M., Fisher, D. and Illingworth, G. 1992 *ApJ Lett*, 400, 1,5.
- Rubin, V. 1994 *AJ* 107, 173.
- Rubin, V. 1993 *Mercury Magazine*, 22, 109 (July / August 1993).
- Rubin, V., Graham, J. and Kenney, J. 1992, *ApJ Lett*, 394, 1,9.
- Sawamura, M. 1988 *PASJ*, 40, 279.
- Sellwood, J. and Merritt, D. 1994 *ApJ* 425, 530.
- Thakar, A. R. and Ryden, B. S. *ApJ* 461, 55.
- Thomasson, M. 1989 Research Report Number 162 Chalmers University of Technology, Gothenburg, Sweden, ISBN 1105564 p. 30-31.
- van den Bergh, S. 1976 *ApJ* 206, 883.
- Walterbos, R. A. M., Braun, R. and Kennicutt, R. C. Jr. 1994 *AJ*, 107, 184
- Zang, T. and Hohl, F. 1978 *ApJ* 226, 521.



## Figure Captions

Figure 1. The evolution of an isolated two-way stellar disk with  $H/D = 0$ . In the figures in this paper, **increasing** darkness levels indicate particle number or mass density in this and the following figures. For more details, see Appendix. Time increases left to right and top to bottom in this and following Figures. Evolution in this Figure is shown at 100 step intervals through 1000 time steps.

Figure 2. The time evolution (left to right, top to bottom) of an isolated one-way stellar disk with  $H/D = 0$  (i. e., disk self gravity is important). Evolution in this Figure is shown at 100 step intervals through 900 time steps.

Figure 3. The evolution of an isolated two-way stellar disk with  $H/D = 0.5$ . Evolution in this Figure is shown at 100 step intervals through 1000 time steps.

Figure 4a. The time evolution of a two-way disk with  $H/D = 1$  perturbed by a 0.1 galaxy mass disturber which passes two disk radii from the center in an orbit co-planar with the disk. The small companion which perturbs the disk edge may be seen in some frames of this and following figures as a black dot in contrast to the lighter colored disk "stars" in those regions.

Figure 4b. The same encounter and two-way stellar disk as in Figure 4a with delineation of the tidal features sharpened by plotting zero velocity dispersion non-colliding particles.

Figure 5. The time evolution of a one-way disk with  $H/D = 1$  perturbed by a 0.1 galaxy mass disturber which passes two disk radii from the center in an orbit co-planar with the disk in the same sense as the disk spin.

Figure 6a. The time evolution of a two-way disk with  $H/D = 1$  perturbed by a 0.1 galaxy mass disturber which passes one disk radius from the center in an orbit co-planar with the disk.

Figure 6b. The same encounter and two-way disk as in Figure 6a with delineation of the tidal features sharpened by plotting zero velocity dispersion particles.

Figure 7. The time evolution of a one-way disk with  $H/D = 1$  perturbed by a 0.1 galaxy mass disturber which passes one disk radius from the center in an orbit co-planar with the disk. The passage is in the same sense as the disk spin.

Figure 8a. The time evolution of a two-way disk with  $H/D = 1$  perturbed by a 0.5 galaxy mass disturber which passes two disk radii from the center in an orbit co-planar with the disk opposite to the disk spin.

Figure 8b. The same encounter and two-way disk as in Figure 8a with delineation of the tidal features sharpened by plotting zero velocity dispersion particles.

11

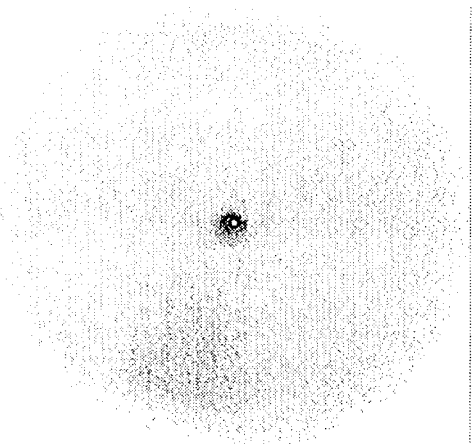
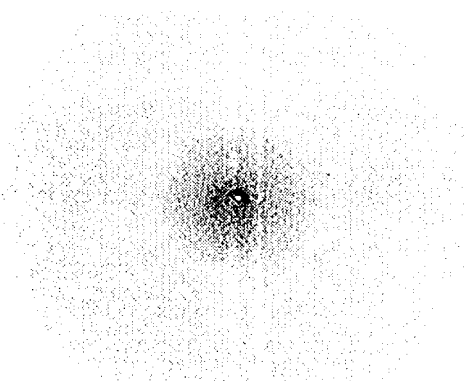
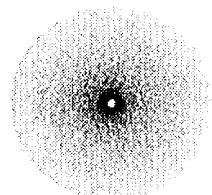
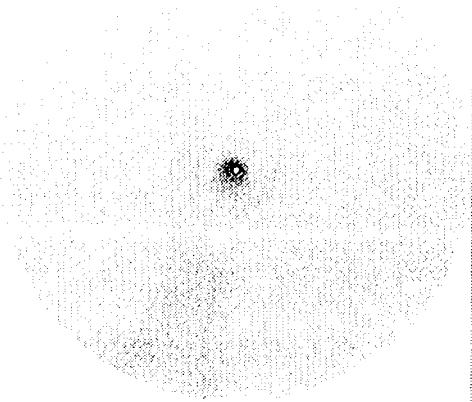
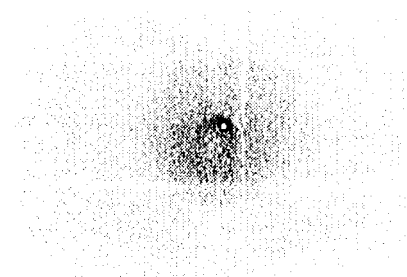
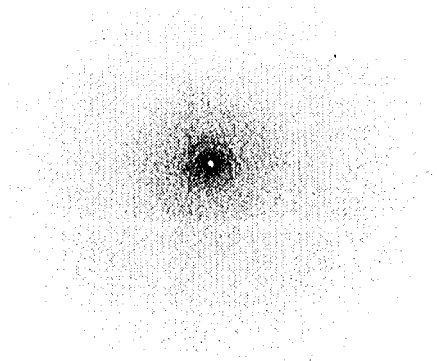
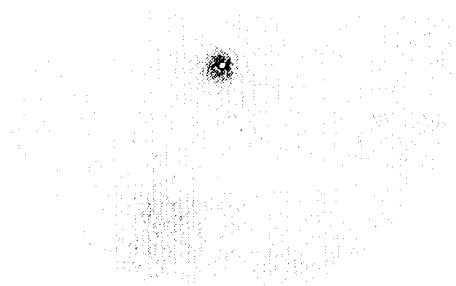
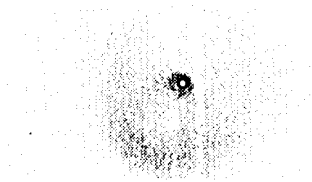
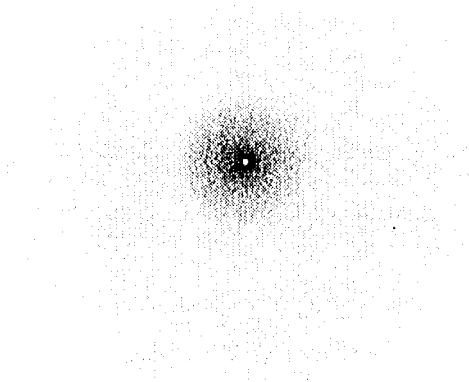
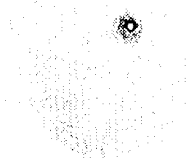
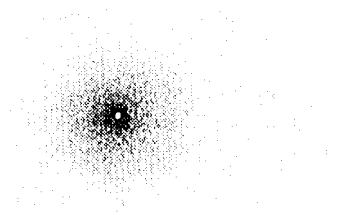
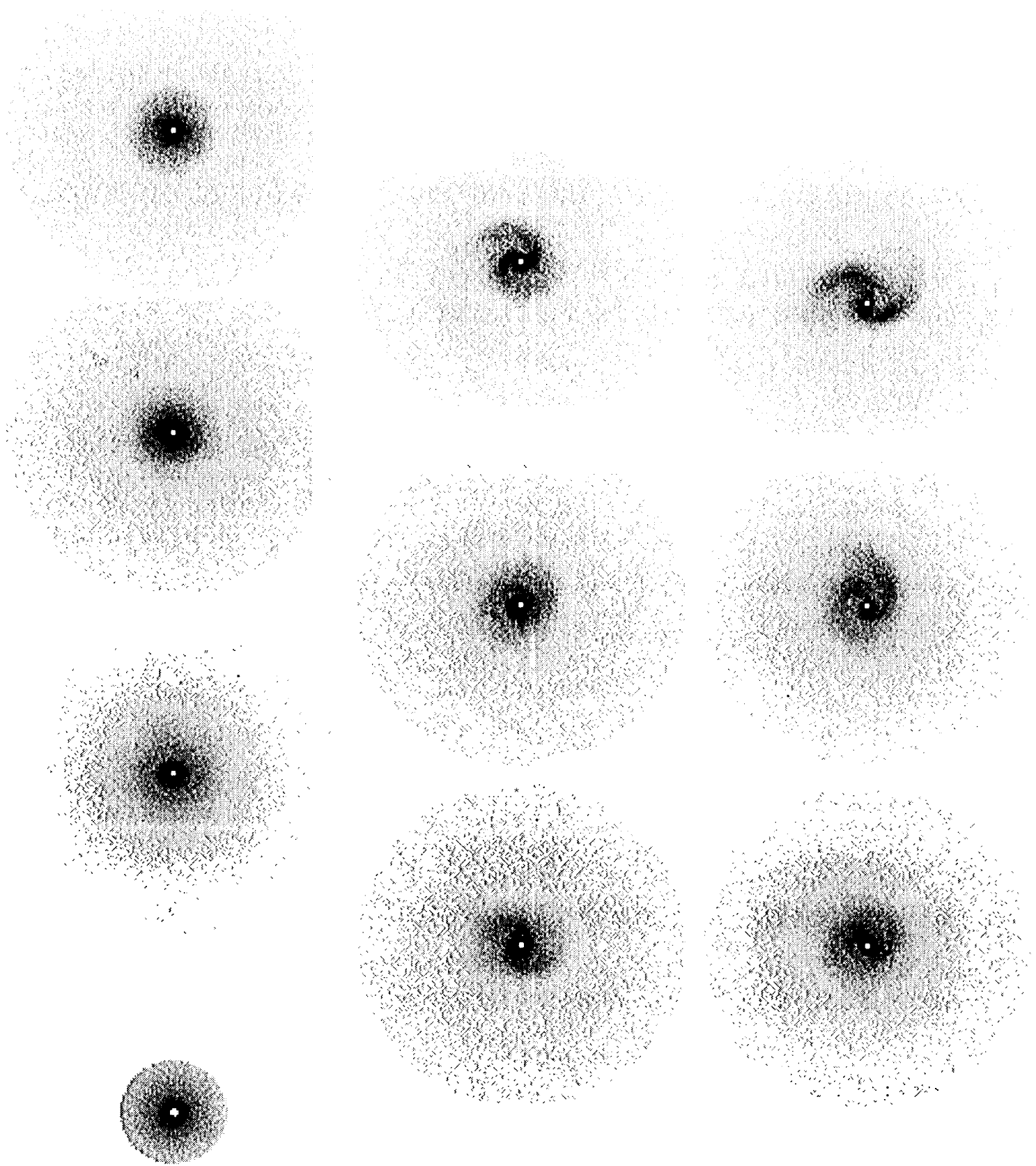


Fig 2



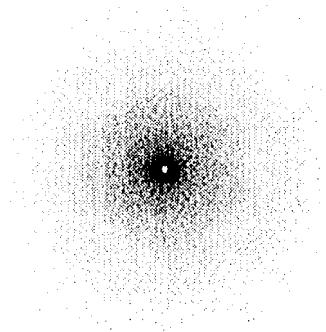
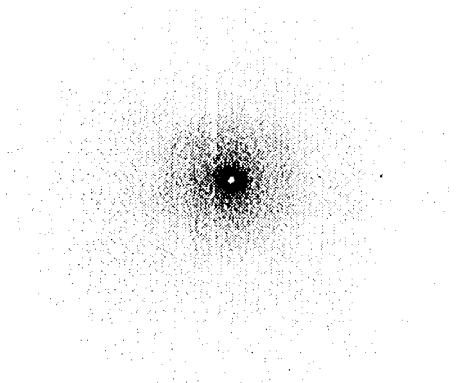
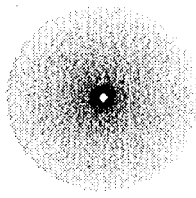
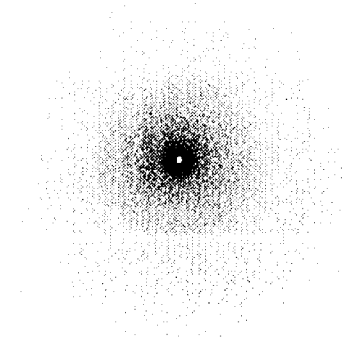
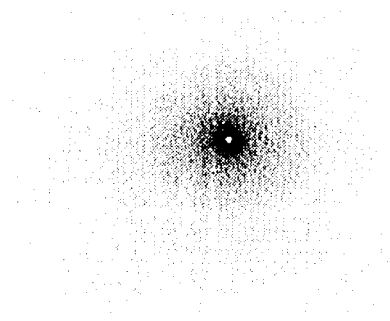
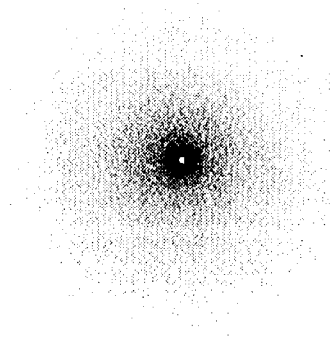
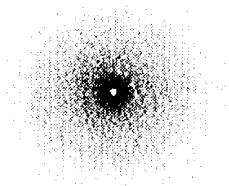
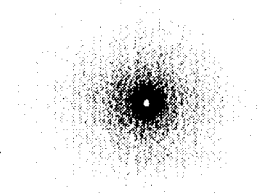
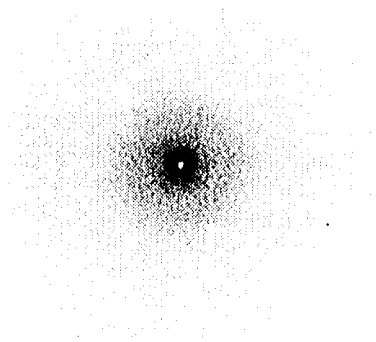
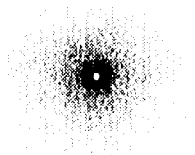
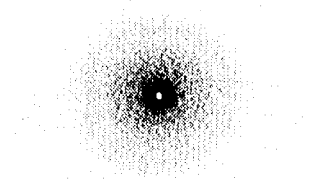


Fig. 1

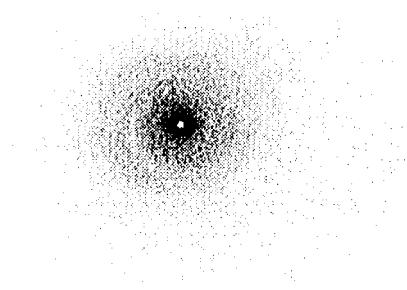
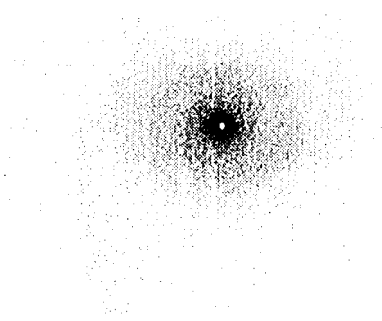
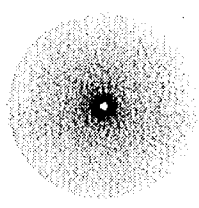
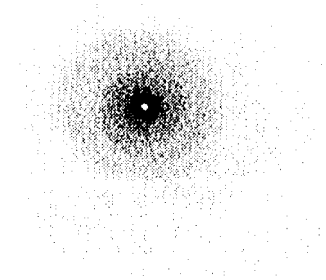
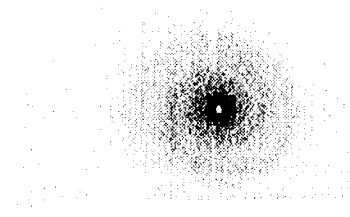
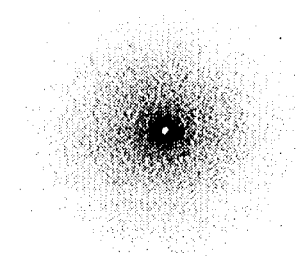
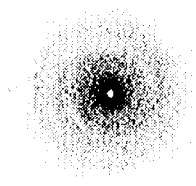
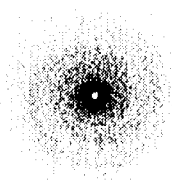
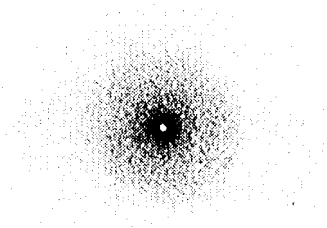
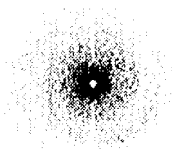
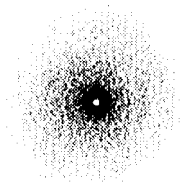
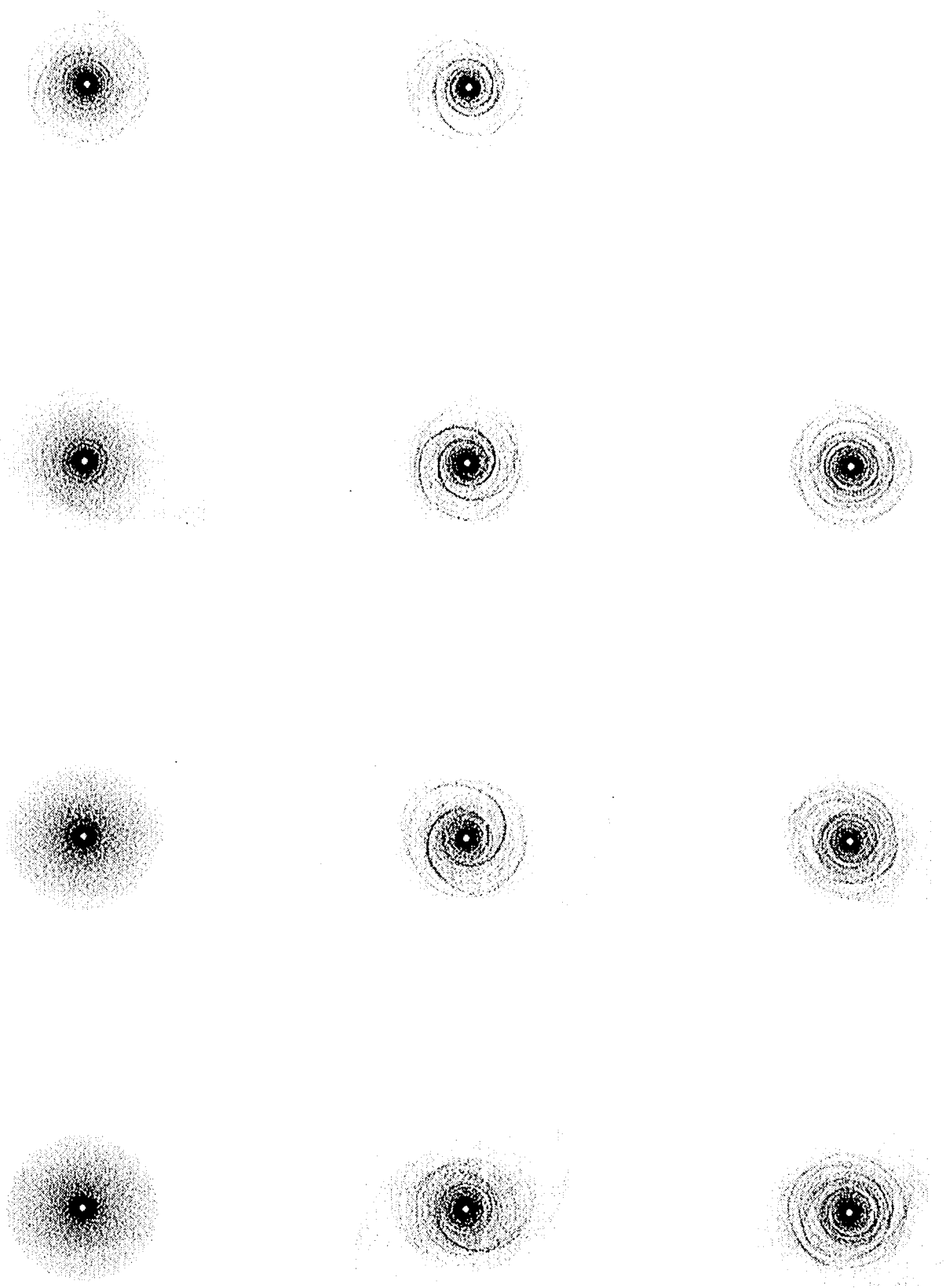
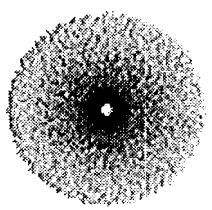
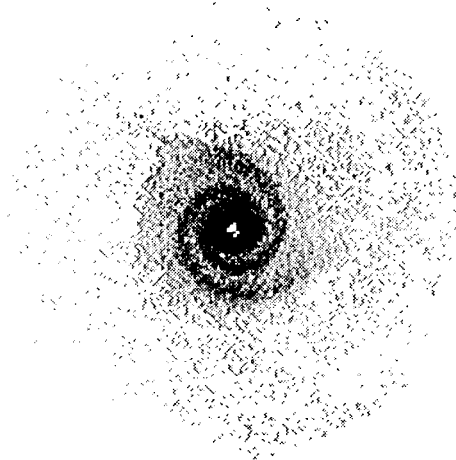
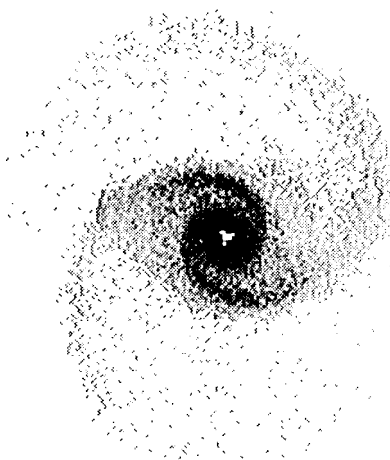
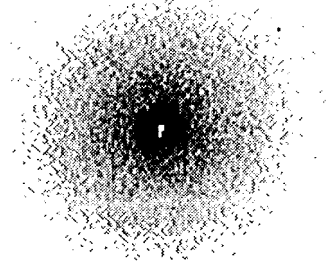
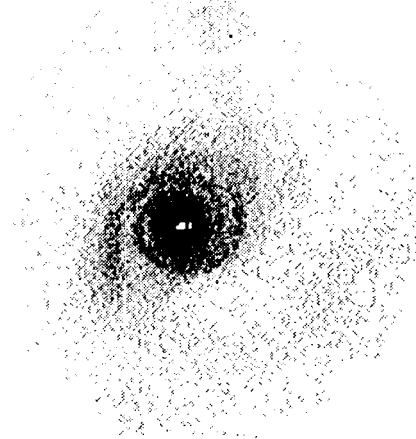
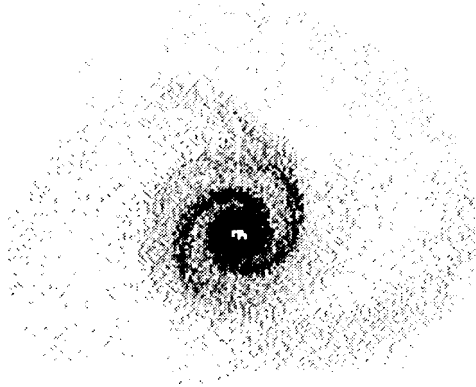
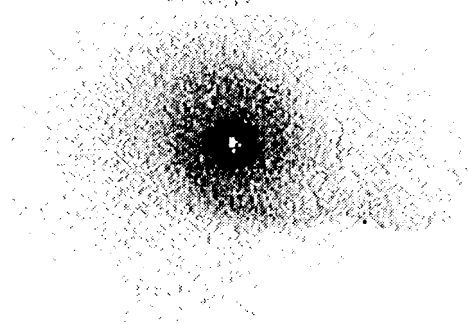
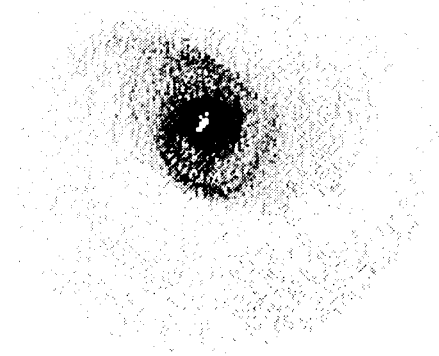
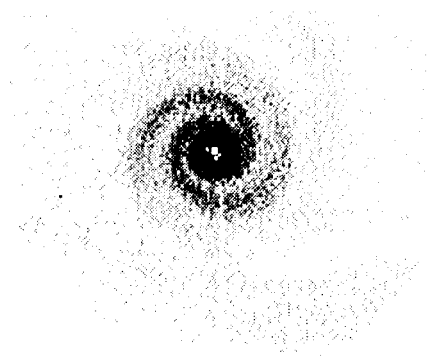
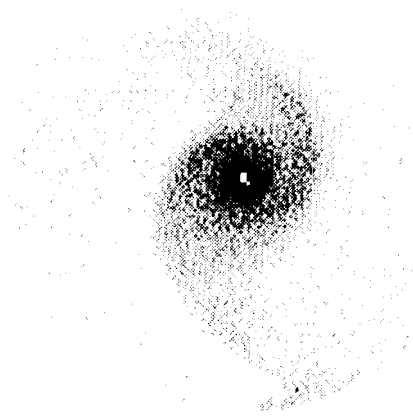


Fig. 4







194

